Landslides (2018) 15:283–296
DOI 10.1007/s10346-017-0871-2
Received: 11 November 2016
Accepted: 31 July 2017
Published online: 15 August 2017

Mirko Carlini · Alessandro Chelli · Roberto Francese · Serena Giacomelli · Massimo Giorgi · Andrea Quagliarini · Andrea Carpena · Claudio Tellini

Landslides types controlled by tectonics-induced evolution of valley slopes (Northern Apennines, Italy)

Abstract This paper investigates the role played by geomorphological and tectonic processes affecting a portion of an active mountain belt in causing the occurrence of different types of landslides developed in flysch bedrock. The adopted multidisciplinary approach (geomorphology, geology and geophysics) allowed to recognize in a portion of the Northern Apennines of Italy different types of landslides that developed in response to slope dynamics, in turn dependent on broader regional-scale tectonic processes. Sedimentary bed attitude, local tectonic discontinuities and lithology only partially influenced the type of landslides, which have been deeply affected by the activity of regional-scale antiform that controlled the hillslope geomorphic evolution in different ways. The growth of this structure and the tilting of its forelimb produced gently dipping slopes that approached the threshold angle that can cause the occurrence of (mainly) translational rockslides. Conversely, high-angle normal faulting parallel to the antiform axis (related to a later stage of activity of the antiform itself) strongly controlled the stream network evolution and caused the watercourses to deeply incise portions of their valleys. This incision produced younger steep valley slopes and caused the development of complex landslides (roto-translational slides-earth/debris flow). The results of the integrated study presented in this paper allowed to distinguish two main types of landslides whose development reflects the events that led to the geomorphological and geological evolution of the area. In this perspective, within the study area, landslides can be regarded and used as indicators of broader-scale recent tectonic processes.

Keywords Landslide types · Tectonics · Slope steepness · Geophysics · Fluvial incision · Northern Apennines

Introduction

The evolution of hillslopes morphology in active mountain ranges has been widely discussed in the last decades and most of the studies analysing these processes are based on the concept that bedrock incision exerted by rivers and torrents in response to tectonic uplift is the main factor controlling hillslope development (e.g. Burbank and Anderson 2011; Larsen and Montgomery 2012; Roering 2012 and references therein). Landsliding in its broadest sense, and not only as a response to fluvial slope undercutting, has also been recognized as an erosional process that can be very effective and play a primary role in active mountain belts (e.g. Crosta and Clague 2006; Korup et al. 2010).

In the Northern Apennines of Italy, large landslides involving bedrock in some cases represent the surface response to the activity of regional-scale uplifted structures (Carlini et al. 2016).

Landslides, and especially their trigger factors, have already been used as indicators of different hillslope processes. Borgatti and Soldati (2010) accounted for landslides as climate change indicators, recognizing enhanced landslides activity during humid and cold periods, triggered by abundant rainfalls and subsequent high hillslopes water-pore pressure. Densmore and Hovius (2000), on the other hand, analysed bedrock landslides occurring on different portions of the hillslopes and argued that earthquake-triggered landslides preferentially develop near ridge culminations (because of the amplification of seismic acceleration at slope crests), while rainfall-triggered landslides are concentrated in correspondence of the toe of the slopes.

In our case, we investigated the possibility of using landslides as indicators of different stages of tectonic structure evolution based on the recognition of different types of landslides developed on different hillslopes, but in response to the same orogenic processes.

In order to do this, we focused our work on flysch-type rocks because of their enhanced capability to preserve features from both geomorphological (erosive landforms, scarps, etc.) and geological processes (faults, fractures, etc.) (e.g. Catane et al. 2007; Chigira 2011).

The study of the relationships between landslides and geological characters of flysch rocks has been long explored in terms of structural control on the type of landslides and of causes and triggers of landslides acting on highly unstable and steepened slopes (e.g. studies on the Flysch Carpathian mountain belt, Záruba 1922; Margielewski 2006; Hradecký and Pánek 2008; Pánek et al. 2008; Šilhán et al. 2014). Possible genetic relationships between these factors and the geomorphological (slope steepness and overall shape) and geological characters (lithology, bedding attitude, folds, faults and fractures) of the bedrock are complex and need to be studied adopting a multidisciplinary approach.

In the Northern Apennines of Italy, where the relationships between geological features and landslides have been indirectly taken into account (Bertolini and Pellegrini 2001; Bertolini et al. 2005; Borgatti et al. 2006), flysch-type rocks (comprised of deeply tectonized marly limestone or siliciclastic sandstone layers that alternate with marls, claystones or shales) are very diffuse (fig. S1) and often involved in large landslides. We selected an area of the Northern Apennines characterized by a uniform lithologic and tectonic framework (Mt. Caio carbonate flysch, representative of many flysch-type lithologies in the overall mountain belt), where different types of large landslides developed. The study of this portion of the chain proved suitable not only to investigate the aforementioned local factors and relationships, but also provided the opportunity to understand the landslide development in relation to processes acting at the scale of the whole valleys (e.g. slopes morphology, stream network evolution, recent tectonic evolution).

The current study took into account three case studies that belong to the same geomorphological and tectonic framework, but that show important differences mainly in terms of type of movement (i.e. translational vs rotational rockslides). Since a connection between this framework and the evolution of some large complex and translational rockslides within the study area has been already established (Carlini et al. 2016), we investigated

the causes of these three different cases, developed within an apparently homogeneous framework.

The partial reactivation in 2013 of Musiara rotational rockslide, the first case study that involved bedrock undergoing failure for the first time gave us the chance to better observe the relationships between bedrock characters and landslide development and movement. The second case study describes the Ripe di Martino landslide, taken into account because: (a) it represents a rotational rockslide developed within the same geological and geomorphological framework of Musiara landslide and (b) its recent activity is constrained by radiocarbon datings.

The third case study is represented by the Carobbio landslide, one the best and largest examples in the region of a complex of translational rockslides located on the right flank of the Parma valley, few kilometres NW of the other cases.

The aim of this work has been to:

1. characterize, for each case study, the geomorphological and tectonic framework and the slope setting (one of the main predisposing factors of landslides occurrence);
2. understand the weight and role played by these characters in relationship to the development of different landslide types;
3. explore the significance of different landslide types within a larger geomorphological and geological framework and use this classification as a proxy for the geological and geomorphological evolution of the area.

We adopted a multidisciplinary approach integrating geomorphological and geological field data, geophysical data (seismic velocity and electrical resistivity) and digital terrain model (DTM)-based geomorphometric analysis of stream basins and drainage network.

Regional setting

The study area is characterized by the outcrops of the Mt. Caio flysch, one of the widest-exposed flysch-type geological formations in the Northern Apennines, reaching a total thickness of at least 1600 m (Cerrina Feroni et al. 2002 and references therein). The Late Cretaceous Mt. Caio turbidites are characterized by thick to very thick carbonate-rich layers alternating with centimetre-thick fine-grained silt-rich layers. From a lithological point of view, the upper portion of the Mt. Caio flysch shows a higher percentage of pelitic fraction with respect to the carbonate beds (Abbate and Sagri 1967). This lithologic characteristic has geomechanical implications, in terms of layers' competence that allow to refer to this formation as a weak rock mass (fig. S2, Mandrone 2004). Within the study area, the Mt. Caio flysch is stratigraphically overlain by the Paleocene-Eocene Tizzano pink marls formation, constituted by carbonate-rich and marly turbidite deposits.

The deformation affecting the Mt. Caio flysch is complex and characterized by multiple phases that developed since the age of its deposition (Late Cretaceous) until the Quaternary. The most recent (Pliocene–Pleistocene?) deformation of the Mt. Caio flysch is mainly represented by high-angle extensional faults and related fractures. The orientation of the recent tectonic lineaments affecting the area is also influenced by regional-scale transpressive structures, such as the one observed on the left side of the Parma valley (Perego and Vescovi 1991).

The combined activity of the two aforementioned tectonic regimes led also to the development of recent regional-scale antiforms, caused by the deep contractional tectonics and dissected by shallow extensional faults (Carlini et al. 2016). In particular, the axial plane of one of the largest antiforms (Ghiare antiform, extending from NW to SE for more than 70 km) crosses the study area by the Mt. Caio (1584 m above sea level—a.s.l.), where the flysch rocks, lying on the forelimb of the antiform, acquire a N-NE-dipping monocline setting. The attitude of the flysch bedding planes controls the geometry of several topographic features within the study area. Wide surfaces with low angle roughly coincide with dip slope attitude, while scarps are located in correspondence of deep incision or counter-dip slope attitude.

Flysch rocks, within the study area, are mainly affected by earth flows (fig. S3a) and complex landslides (fig. S3b) (Borgatti et al. 2006, Carlini et al. 2016, Bertolini et al. 2017). Earth flows are often characterized by multiple sources of material, involving slope deposits or bedrock constituted by clay-rich or marly facies of flysch-like rocks. These landslides have an elongated and narrow main track and a fan-shaped accumulation zone. Large complex landslides often show a unique source area where the failure surface deepens in the bedrock. The depleted rock masses slide down the slope, usually as a unique block. At the toe of the landslide, the type of movement evolves into a flow because of the great amount of fine-sized (pelitic) material and water. From a geomorphological point of view, these kinds of landslides are characterized by concave to convex landforms related, respectively, to the depletion zone and the deposit. In the studied area, huge rockslides are both translational and rotational. The translational slides occur where gently dipping slopes exist, while rotational ones prevail where the slopes are steeper. Large landslides affecting relevant portion of slopes composed of flysch rocks usually undergo partial, or seldom total, reactivations characterized by different types of movement. In some cases, they increase their volume through retrogressive and/or advancing and/or enlarging distribution of activity.

The geological (lithology, structure, tectonics) and geomorphological (slope morphology, steepness, erosive processes) characteristics represent the main predisposing factors invoked for the landslides in the Northern Apennines (Bertolini et al. 2005; Bertolini et al. 2017) mainly because they are responsible for the lower rock mass quality and rock strength. These conditions depend also on lithological factors, such as in the case of flysch rocks, which are characterized by the alternation of beds with very different geomechanic properties (e.g. limestones and marls or claystone, sandstones and shales). Besides, weathering, mainly of physical type, contributes to weaken the rocks as well (Bertolini and Pellegrini 2001).

Also, climate factors contributed as trigger and/or predisposing factors to landslide occurrence. In fact, during the Last Glacial Maximum (LGM), glacial and periglacial climate conditions affected a large portion of the Northern Apennines (Giraudi 2011; Federici and Tellini 1983). At that time, the valley of the Parma Torrent and of the close Cedra Torrent hosted mountain glaciers, which led their snouts along the valley bottom few kilometres southwards from the investigated area. The equilibrium line altitude (ELA), calculated employing lateral and frontal moraines (Federici and Tellini 1983), lied at about 1250 m a.s.l. (Fig. 1a). Therefore, all morphologically suitable topographic surfaces above

this altitude could potentially host a glacier or, at least, a glacieret or a perennial snowfield, like the spoon-shaped area north of the Mt. Caio (Fig. 1a). As suggested by the landforms and the position of the ELA, though, glaciers did not cover the ground surfaces interested by the landslides treated in this paper, where mostly periglacial processes, like frost shattering and freezing and thawing, widely contributed to the physical weathering of rock masses (Bertolini and Pellegrini 2001). In particular, the transition from glacial-periglacial (dominated by frozen water) to paraglacial (dominated by liquid water) conditions favoured snow and ice melting that may have contributed to the increase in porewater pressure in the slopes, possibly favouring rock slope failures, as suggested by McColl (2012). Thawing of permafrost ice in ice-bonded joint networks may have enhanced joint water pressures during deglaciation, contributing to further lower the rock mass quality. These extrinsic mechanisms, though, are usually not ubiquitous trigger factors for rock slope failures in deglaciated areas (Ballantyne et al. 2014).

Climate conditions still control the present-day main trigger factors of the landslides, represented by heavy and prolonged rainfalls occurring mainly in autumn and in spring, partially associated with the snowmelt (Bertolini and Pellegrini 2001; Chelli et al. 2006). Large part of the phases of activity of landslides recorded in the area grew during the rainiest periods of the Holocene (Bertolini et al. 2005). Trigger factors are sometimes represented also by the undermining of slopes caused by the stream banks erosion during the floods and, more rarely, by seismic shocks (Tosatti et al. 2008). Several landslides affected the study area, mainly as partial reactivation of more ancient landslides and, in some circumstances, also involving the undisturbed bedrock.

Methods

A DTM with 5 m of geometric resolution (Regione Emilia Romagna Topographic Database) was employed to investigate the geomorphological and structural features of the study area.

Our work is based on an updated version of the Regione Emilia Romagna landslides inventory (Servizio Geologico, Sismico e dei Suoli della Regione Emilia-Romagna 2014), in which the landslides have been reviewed and classified according to Cruden and Varnes (1996). The geomorphological characters of the landslides have been identified through satellite image analysis and field surveys in order to recognize their type and distribution.

Structural field data (joints and fractures) have been collected at 11 structural stations and integrated with the structural data from the published geological maps and the DTM structural analysis in order to obtain a full data coverage of the area of interest (Fig. 1). Some of the structural stations were located at outcrops close to the studied landslides, in particular:

- Stations 3, 4, 8—Carobbio landslide;
- Station 7—Musiara landslide;
- Station 10—Ripe di Martino landslide;
- Stations 1, 2, 5, 6, 9, 11 complete the coverage of the study area.

Fracture orientation and bedding have been collected at each station.

Geophysical imaging at the Musiara site was a major aid to explore the relationships among geometry of landslide body, bedrock and tectonic features. We used both shallow boreholes and bedrock outcrops to constrain and calibrate the geophysical interpretation of electrical and seismic data. The resistivity model was generated via 3D inversion with an iterative procedure based on the smoothness-constrained implementation (Constable et al. 1987) associated with a careful reweight of the inversion parameters (Morelli and LaBrecque 1996). Cells with depth of investigation (DOI) value larger than 0.2 (Oldenburg and Li 1999) were not considered for interpretation. The velocity model was obtained via the classical traveltime tomography approach (Vesnaver 2013). Inversion was carried out with the simultaneous iterative reconstruction technique (SIRT) algorithm. The difference between real and calculated arrivals was lower than 5% for most of the rays. Cells initialized with a velocity values but not crossed by rays were not considered for interpretation.

The geomorphometric analysis, performed under GIS environment, has been used to reconstruct the drainage network and the slopes morphological evolution of the Parmossa valley, where the two studied rotational rockslides are located. The incision map of Fig. 2b represents the local relief, calculated as the difference between maximum and minimum elevation inside a moving window of 150 m × 150 m (Ciccacci et al. 1992; Centamore et al. 1996; Mumipour and Tahmasabi Nejad 2011 and references therein; Shahzad and Gloaguen 2011). The stream length (SL) gradient index has been calculated to quantify the perturbations along the Parmossa Torrent longitudinal profile because of its sensitivity to minimum slope variations (Troiani and Della Seta 2008; Burbank and Anderson 2011; Gao et al. 2013). This index is mainly influenced by important lithological variations, sediment discharge by tributaries, tilting, faults and landslides interfering with the stream profile and/or thalweg. According to the formula suggested by Hack (1973), the SL has been calculated keeping a fixed horizontal length (ΔL) of the segments of 150 m.

Results

The structural analysis of the DTM highlighted the orientation of tectonic features that are associated with landforms recognizable within the resolution of the DTM. Five main groups of discontinuities have been recognized, with average directions N290°, N345°, N60°, N360° and N90°, as shown by the rose diagram of Fig. 1b. The field structural data related to stations 1, 2, 5, 6, 9 and 11 suggest the presence of five main families of discontinuities whose orientations are comparable with the directions of the aforementioned lineaments (compare the two rose diagrams in Fig. 1b).

Morphologic analysis of the hillslopes

The three landslides studied developed on two types of slopes presenting different geometrical characteristics, such as shape and angle. The Musiara and Ripe di Martino landslides developed on the left side of the Parmossa valley, while the Carobbio landslide lies on the right side of the Parma valley (Fig. 1).

The analysis of the geomorphological profile of the hillslopes revealed that moving upstream (southward), both Parma and Parmossa valleys slopes are initially symmetrical and quite smooth (profiles A and B, Figs. 1b, and 2a). On the contrary, in profiles C and D (Figs. 1b and 2a), closer to the Ghiare antiform axis, and where the studied landslides are located, both valleys show significant morphological changes and present evident slope breaks.

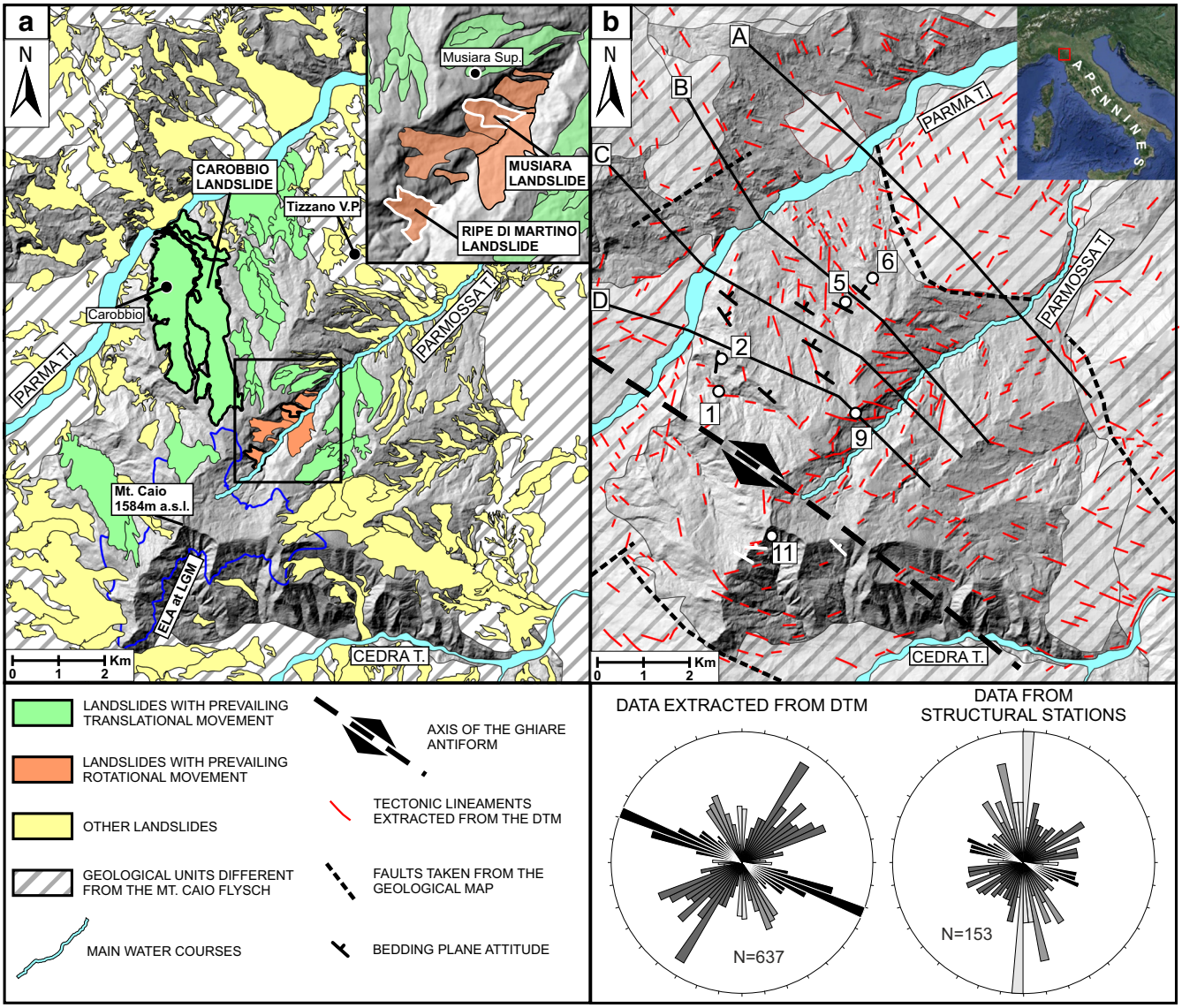

Fig. 1 **a** Sketch map of the studied area where prevailing translational rock lides (Carobbio-type landslides) and prevailing rotational rockslides (Musiara-type landslides) are highlighted; *zoom in the top right corner* shows the Parmossa valley where the Musiara and Ripe di Martino landslides are located. **b** Tectonic and structural features of the investigated area; *black solid lines labelled A, B, C* and *D* are the traces of topographical profiles of Fig. 2a. The *rose diagrams* show the orientations of the linear tectonic features extracted from the 5-m-resolution DTM (*left diagram*), and the orientations of the joints collected at the *numbered* structural stations

Concerning the valley of the Parma Torrent, along profiles C and D, the lower portion of the slopes is highly asymmetrical with respect to the watercourse, much steeper on the right side, where SW-NE-oriented faults and the anti-dip slope bedding attitude of the Mt. Caio flysch control the slope geometry (Fig. 1b). Along this lower portion of the slope minor rock falls, shallow debris flows and rock/debris slides develop. The upper portion of the Parma Torrent right slope, on the contrary, is characterized by a relatively lower angle and an irregular surface, caused by the dip slope bedding attitude, the presence of the Carobbio landslide and some fault scarps (Figs. 1 and 2a). The Parmossa valley slopes, conversely, show a symmetrical geometry (profiles C and D), characterized by high angles and abrupt breaks that suggest upstream deepening processes, as it is also clearly visible in map view (Fig. 1b). Both sides of this part of the Parmossa valley are dominated by

Fig. 2a Topographical profiles (5-m-resolution DTM, traces on Fig. 1b) across the Parma and Parmossa valleys. The profiles are ordered moving upstream from north (*A*) to south (*D*). The attitude of Mt. Caio Flysch bedding and cross-section of landslides are reported, respectively, following the results of geological and geomorphological fieldwork. The *thick black solid line* in profile *C* and *D* represents the Parmossa valley sides in correspondence of its incised portion (area 1 of Fig. 2b, c). **b** Incision map—*black lines* highlight zones of higher incision degree. *Solid lines* (*numbered 1*, *2* and *3*) indicate zones of incision related to local stream dynamics; *dashed lines* indicate incision related to structural features. **c** Zoom on zone 1 of Fig. 2b and on the headwater area of the Parmossa Torrent (bounded by the *dotted line*). **d** SL index curve (*black solid line*) plotted over the longitudinal profile (*grey line*) of the Parmossa Torrent. *Black dots* represent the knickpoints of the stream

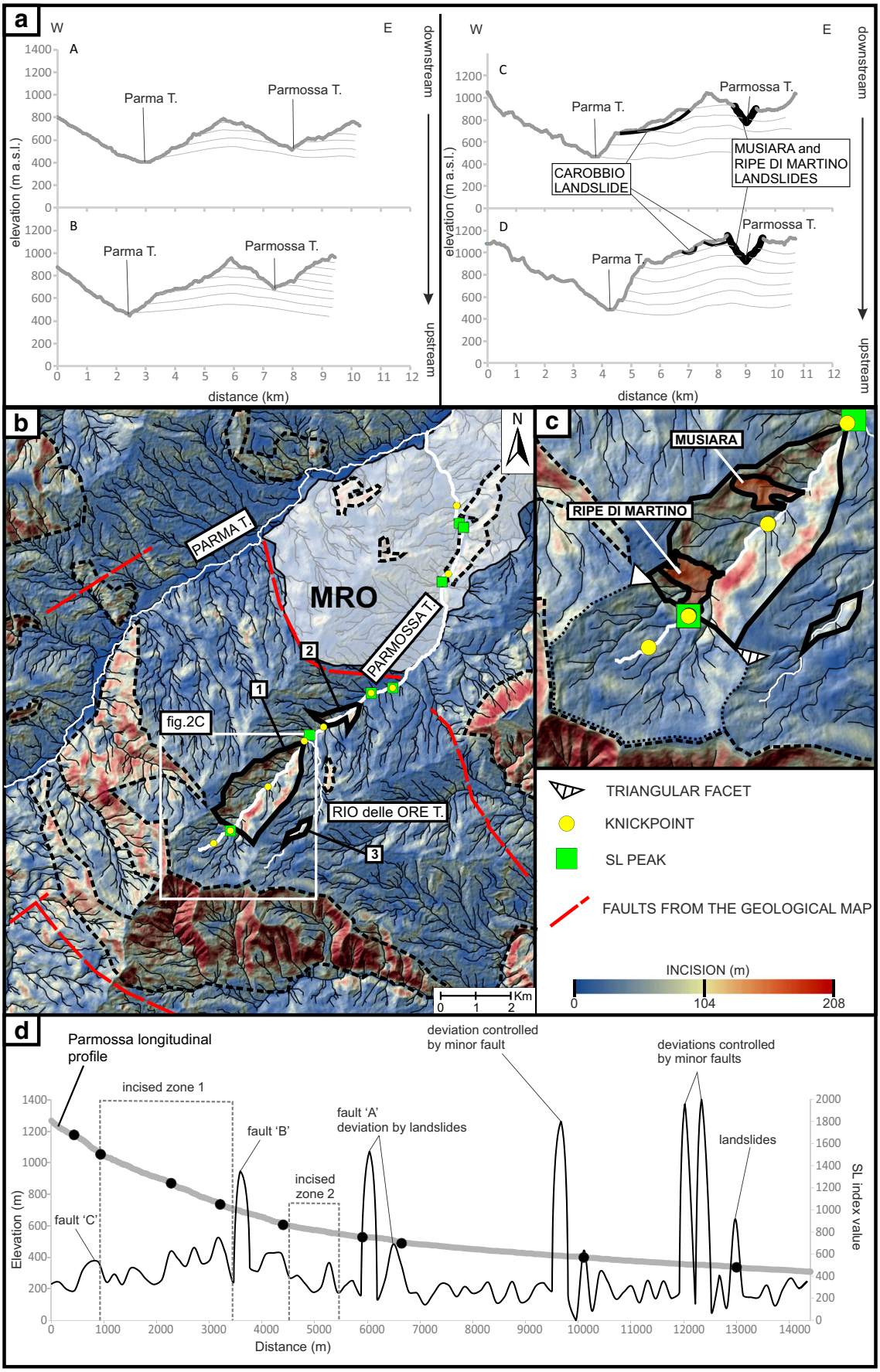
a
W
E
A
Parma T.
Parmossa T.
B
Parma T.
Parmossa T.
elevation (m a.s.l.)
distance (km)
downstream
upstream
C
Parma T.
Parmossa T.
CAROBBIO LANDSLIDE
MUSIARA and RIPE DI MARTINO LANDSLIDES
D
Parma T.
Parmossa T.
b
N
PARMA T.
MRO
PARMOSSA T.
1
2
3
fig.2C
RIO delle ORE T.
Km
c
MUSIARA
RIPE DI MARTINO
TRIANGULAR FACET
KNICKPOINT
SL PEAK
FAULTS FROM THE GEOLOGICAL MAP
INCISION (m)
d
Parmossa longitudinal profile
incised zone 1
fault 'B'
fault 'A'
deviation by landslides
deviation controlled by minor fault
deviations controlled by minor faults
incised zone 2
fault 'C'
landslides
Elevation (m)
SL index value
Distance (m)

landslides with prevailing rotational movement, as in the case of the Musiara and Ripe di Martino landslides.

Geomorphometric analysis

We performed a geomorphometric analysis of the Parmossa drainage basin in order to explain the development of the incised portion of the Parmossa Torrent that has been highlighted by the DTM and slope analyses. We analysed and integrated data related to the local relief energy, the drainage pattern, the stream longitudinal profiles and the SL gradient index (or Hack's index; Hack 1973).

The incision map of Fig. 2b shows zones characterized by high local relief energy that in most cases are located in correspondence with major structural and/or tectonic features, such as scarps characterized by anti-dip slope bedding attitudes and fault scarps (dashed lines in Fig. 2b, compare with Fig. 1b). Three of these zones, nonetheless, represent deeply incised areas of the Parmossa and Rio delle Ore Torrent basins (solid lines in Fig. 2b), characterized by a symmetrical shape with respect to the watercourses. The Parmossa Torrent widest incised area (area 1 in Fig. 2b, c) hosts the Musiara and Ripe di Martino landslides and it is bounded to the southwest by a sharp and straight transition to a zone showing a relatively lower degree of incision, where the present-day stream headwater is located (dotted area in Fig. 2c).

The comparison between the Parmossa Torrent longitudinal profile and the SL curve highlights that the highest SL peaks approximately coincide with the torrent knickpoints (Fig. 2c, d). As a general rule, differential erodibility due to lithology changes as a cause of the SL peaks along the Parmossa Torrent can be reasonably excluded because the only relevant lithological change (between Mt. Caio flysch and Tizzano pink marls) is controlled by a NE-dipping normal fault. Important confluences of streams with a significant discharge flowing into the Parmossa Torrent are also lacking. Therefore, the factors interfering and affecting the watercourse (highlighted by the SL index) are likely to be mainly the presence of landslides reaching the riverbed and/or tectonic features (Fig. 1). Moving downstream along the profile, the first two relevant peaks in the SL index delimit the incised portion of the basin (zone 1 in Fig. 2b), which seems to widen the upstream, from north to south. This zone is also characterized by a convex trend in the shape of the stream longitudinal profile. The lack of other landforms and landslides interfering with the riverbed suggest that both these SL peaks are reasonably related to tectonic features.

In the case of the first SL peak, in particular, the presence of clear NE-dipping triangular facets suggests that the tectonic control may be represented by a normal fault (fault 'C' in Fig. 2d) oriented in the same way that may constitute the sharp boundary between the incised portion and the southward neighbouring area (dotted area of Fig. 2c). The latter is characterized by a very low slope, an almost convex topography and a poorly developed drainage network showing evidences of incipient incision. Also, the second SL peak is likely to be connected to the presence of a fault, whose morphological evidences are mainly represented by slope breaks along the Parmossa Torrent watershed (fault 'B' in Fig. 2d). Other two SL peaks occurring downstream the aforedescribed area correspond to an evident eastward change in the torrent flow direction caused by active large landslides (mainly earth flows) affecting the western side of the Parmossa valley and reaching the riverbed (Fig. 1a). Besides, the NE-dipping normal fault (fault 'A' in Fig. 2d) constituting the contact between the Mt. Caio flysch and the Tizzano pink marls crosses the valley just nearby the deviation of the stream direction. Therefore, it is difficult to assess which of these factors mostly influence these SL peaks. Other relevant SL peaks further downstream are all related to stream local deviations caused by minor faults and landslides reaching the valley floor. Apparently, these processes do not seem to produce any relevant incision effect on the valley sides, probably due to the greater erodibility degree of the outcropping lithology (Tizzano pink marls) in this area, which is not the object of the present study.

Musiara landslide

The Musiara landslide is located on the left side of the Parmossa valley and its' name is derived from the close village of Musiara, which includes two separated settlements (Musiara superiore and Musiara inferiore) (Fig. 3). Southwards of Musiara superiore, some scarps with an approximate NE-SW direction show an arcuate shape in map view. Along the slope below these scarps, slabs of marly limestone with a nearly horizontal attitude or slightly tilted backward, can be observed. These slabs are derived from beds outcropping upslope subsequently detached by rotational rockslides. These rockslides have been reworked by different successive landslides, as can be deduced from the cross-cutting relationships among the landforms (Fig. 3a). The last of these landslides occurred between 10 and 11 April 2013, and moved from WNW to ESE (Fig. 4). The top of the landslide scarp is 980 m a.s.l. and the tip is 810 m a.s.l., and the latter reached the thalweg of the Parmossa Torrent. The main scarp is characterized by a variable height ranging from 40 to 15 m. The thickness of the landslide deposit is maximum in correspondence of its head, while it becomes thinner towards its foot. Centimetre-to-decimetre scars and striae characterize the rocks constituting the surface of rupture that crops out where the landslide deposit downslope gradually thins. These geomorphological features reveal that the Musiara landslide was a dominantly rotational slide where the shear surface developed in part along and in part cutting several beds of flysch.

Musiara landslide shows the coincidence of morphological elements (flanks and some portions of the main scarp) with the tectonic features highlighted by the structural data. In particular, the main scarp is likely to be controlled by the N-S systems of fractures and faults, while the flanks of the landslides are controlled by the WNW-ESE-oriented tectonic features, as highlighted also by the seismic lines L2 and L4B (Figs. 3b and 5c, d). The orientation of the fractures has been collected in one structural station located NE of the landslide (station 7) (Fig. 3a). At station 7, the Mt. Caio flysch bedding is quite regular, constituting a NE-dipping monocline, not affected by folding or major faulting. The joints can be grouped in three main families whose average directions are ~ N50°, ~ N120° and ~ N160° that fit the directions of the main tectonic features highlighted by the DTM analysis (Fig. 1b).

Resistivity in the imaged volume of the landslide deposit ranges from 5 Ωm to values larger than 250 Ωm. The cross-section shows alternating resistive and conductive domains (Fig. 5a). Topography along the profile is also shaped as a staircase with dipping segments alternated to almost flat segments. Higher gradient slopes correspond to resistive terrains while gently dipping slopes

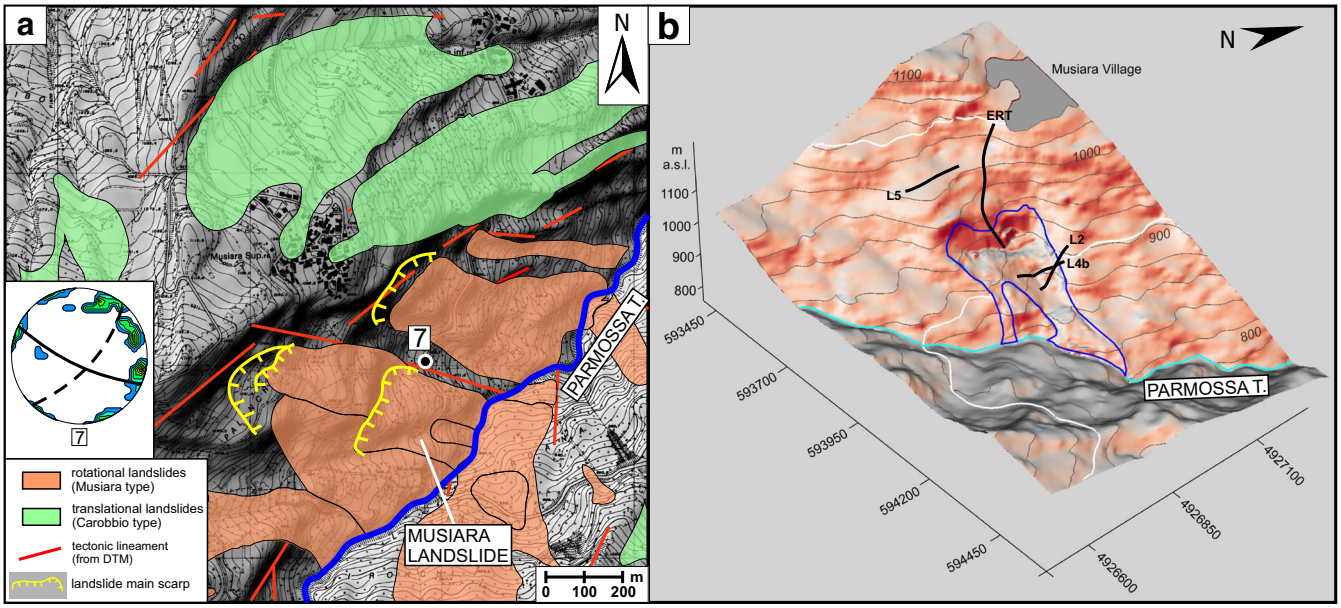

Fig. 3 **a** Sketch map of Musiara landslide area. The *stereonet* represents the contours of the poles related to the joints orientation. *Black solid line* indicates orientation of the Musiara landslide flanks; *black dashed line* indicates orientation of the Musiara landslide scarp. **b** 1-m-resolution hillshade representation of the topography after the landslide. *Black solid lines* represent the location of the ERT and seismic lines (Fig. 7)

correspond to conductive units. The upper resistive body ranges from 1035 m a.s.l. down to 1015 m a.s.l. and the bedrock is partly outcropping. The intermediate resistor ranges from 1000 m a.s.l. to about 970 m a.s.l., where the bedrock in this segment is hardly visible. The lower resistor represents the most dipping slope along the investigated profile and the bedrock is outcropping at various spots. The detachment surface of the 2013 landslide developed right into the resistive unit and the top of the failure scarp is located at the elevation of about 980 m a.s.l. Resistive units could also be related to observed outcrops and associated to moderately hard rock layers of the Mt. Caio flysch. The conductive units are quite similar as they comprise the almost flat segments of the profile exhibiting an inclination of less than 5°–10°. Bedrock does not outcrop in the conductive domains, but its top is located few meters below the surface. These domains, based on the very low resistivity values, are probably composed of soft rocks with a relative abundance of silt and clay in the matrix. This fact is consistent with the more pelitic lithofacies recognized in the upper part of the Mt. Caio flysch (Abbate and Sagri 1967).

P-wave velocity in profile L5, roughly located on the same gently dipping slope as of the upper conductive domain, ranges from 300 to 2000 m s^{-1} (Fig. 5b). The average P-wave velocity in the near surface layer is about 450 m s^{-1} while it jumps up to 1500–1600 m s^{-1} in the second layer and a third layer exhibits a velocity of about 1900–2000 m s^{-1}. The maximum thickness of the low-velocity uppermost layer is about 10–15 m and it is fully comparable with the low resistivity unit of the ERT profile (Fig. 5a). The low velocity value is typical of soft rocks like marls, silt or clays. Profiles L4B and L2 were collected on the eastern scarp of the landslide (Fig. 5c, d). Both profiles show a high-velocity unit with a flat top just below the surface and at a depth of about 10 m. The P-wave velocity of these units is about 2400–2600 m/s, possibly indicating moderately hard rocks. One of the high-velocity layers is partly exposed at the base of the eastern flank of the landslide, as

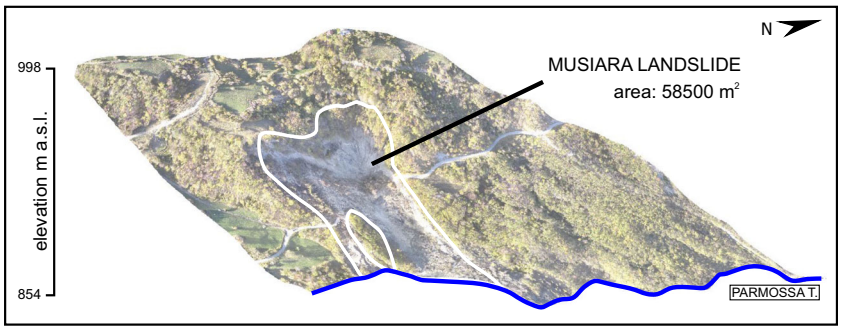

Fig. 4 3D diagram of the reactivated portion of the Musiara landslide occurred in 2013. Elevation is based on a 1-m-resolution DTM on which a drone photo (courtesy of the Parma Province Administration) has been projected

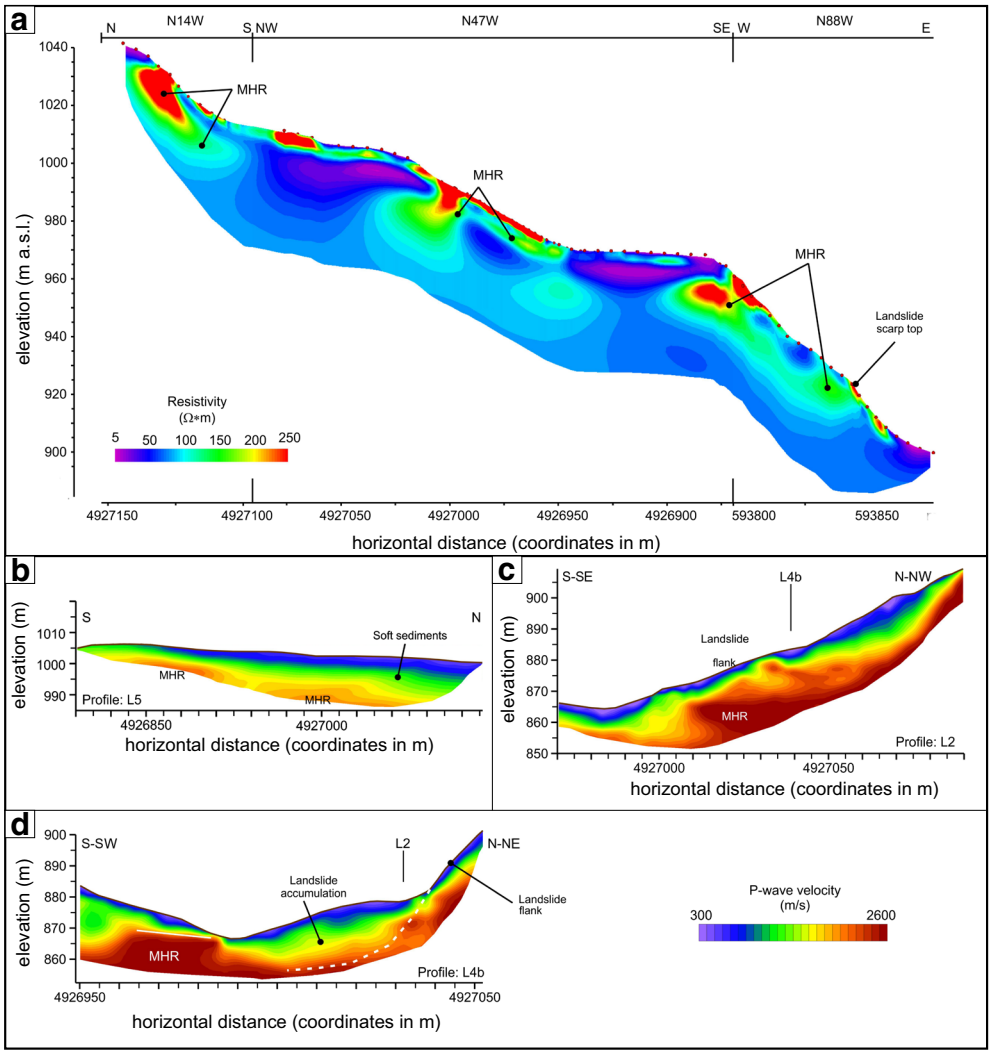

Fig. 5 **a** Electrical resistivity tomography (ERT) performed along the slope of Musiara landslide (trace on Fig. 3b). **b**, **c**, **d**—Seismic profiles performed in the Musiara landslide area (traces on Fig. 3b). The *white dashed line on profile* **d** represents the landslide slip surface. *MHR* moderately hard rocks

it represents the sliding surface. The moderately high p-wave velocity zone on profile L4B is characterized by a lack of lateral continuity and it has been interpreted as not in place and/or part of a pre-existing rockslide. On profile L2, on the contrary, the moderately high p-wave velocity zone is more continuous and interrupted only towards SSE, leading us to interpret it as bedrock. The velocity field in the landslide body is variable as it ranges from 400 to 1500 m s^{-1}. The near surface deposits are characterized by a low velocity also in the eastern flank and in the upper slope, indicating the presence of soft rocks or of backfill material (profiles L4B and L2).

Ripe di Martino landslide

In the area of Ripe di Martino, several features point out the existence of a system of landslides that involved the left side of Parmossa valley (Fig. 6). These are bedrock rotational slides that evolved in debris flows (Fig. 6). The complex of landslides underwent several reactivations and the last landslide occurred in 2000, affecting a portion of an ancient one, as testified by the radiocarbon dating (Table 1) performed on wood fragments involved in this last reactivation (Fig. 7) (Tellini and Chelli 2003; Soldati et al. 2006).

The organic material was recognized as pieces of trees' branches that were collected from the ancient landslide deposit involved in the last reactivation. They were found in two distinct portions of the landslide, dispersed within a clayey matrix and represent the remains of trees involved during two distinct phases of landslide activity (Tellini and Chelli 2003). The reactivation occurred in 2000 started just down-slope a scarp of resistant limestone. The foot of the landslide reached the channel of the Parmossa Torrent. The landslide showed a composite and/or complex style of activity. In the detachment zone, the main failure mechanism is interpreted to be rotational-translational (Fig. 6). The failed mass then broke into a debris mass and the landslide turned the movement in a debris flow, constituted by blocks and clasts of limestone supported by a clayey matrix.

Station 10 is located close to the main scarp left by the detachment of the older portion of the Ripe di Martino landslide (Fig. 6).

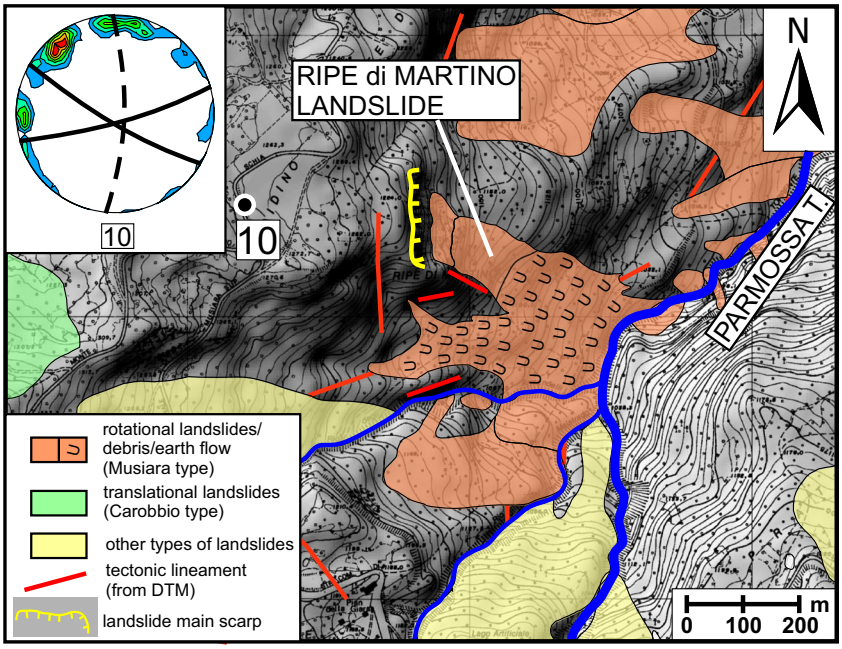

Fig. 6 Sketch map of Ripe di Martino area. The *stereonet* represents the contours of the poles related to the joints orientation. *Black solid line* indicates orientation of the Ripe di Martino landslide flanks; *black dashed line* indicates orientation of the Ripe di Martino landslide scarp

Fracture orientations at structural station 10 are variable, even though three major trends with azimuth N50°, N105° and N170° can be recognized.

Carobbio landslide

In the western portion of the study area, on the right side of Parma valley, the slope of Carobbio is characterized by a large complex of landslides (Fig. 8) that are ancient (as shown by the radiocarbon ages in Table 1) and often subject to several reactivations.

The organic remains used for the ^{14}C analysis were found at different depths of a drilled core. Sample S5, found at − 5 m, was represented by vegetal organic material, probably belonging to palustrine deposits, while sample S4, found at −17.5 m, was represented by wood remains. These data constrain two phases of activity of a translational rockslide constituting a portion of the whole complex of landslides (Tellini and Chelli 2003).

This landslide is characterized by a detachment zone located at an elevation of about 1130 m a.s.l. and involves the Carobbio village. It underwent several reactivations during the last two centuries. The main phases of activity occurred on 3 April 1855, when the village was destroyed, and, again, on 6 June 1900. The large landslide in the eastern portion of the area is dormant and its detachment zone is located just below Mt. Pesdonica (1300 m a.s.l.), while its' foot reaches the channel of the Parma Torrent (Fig. 9). Both the right and left flanks of the landslide are NNW-SSE oriented and they are delimited, in the upper part of the slope, by two scarps shaped in the outcropping rock. This landslide has some portions that show an intermittent activity characterized by a very slow rate of movement. In general, all these landslides are translational rockslides, as testified by the overall geomorphological features (detachment scarps and flanks, linear trenches in crown areas). In some cases, they are rock block slide, such as the landslide involving the still-inhabited portion of Carobbio village. Besides, different rock blocks slid one on the other at different times.

At structural stations 3, 4 (in the outcrops bounding the landslide) and 8 (outcrop close to the main scarp of the landslide), the joints can be grouped in two main families oriented ~ N170° and ~ N80° (Fig. 8). At these stations, even though fracture orientation variability is quite high, conjugate sets related to the two main families of discontinuities can still be observed. Also, the analysis of the Carobbio landslide shows the existence of a tectonic control over the development of the landslide elements.

Discussion

In all of the three case studies, the orientation of the landslides scarps and flanks is controlled by recent tectonic discontinuities such as fractures and faults. These features are in agreement with

Table 1 Radiocarbon datings of Ripe di Martino and Carobbio landslides (Soldati et al. 2006; Tellini and Chelli 2003)

Sample	Lab code	^{14}C age yearBP	2σ Cal yearBP	$^{13}C/^{12}C$ (‰)	^{14}C conv. yearBP
Le Ripe 1	Beta 166793	2260 ± 60	400–170	− 25.2	2250 ± 60
Le Ripe 2	Beta 166794	5360 ± 70	4340–3980	− 25.9	5340 ± 70
Carobbio S4	Beta 151582	25,129 ± 160		− 26.6	
Carobbio S5	Beta 151583	17,330 ± 110	21,200–20,060	− 26.3	

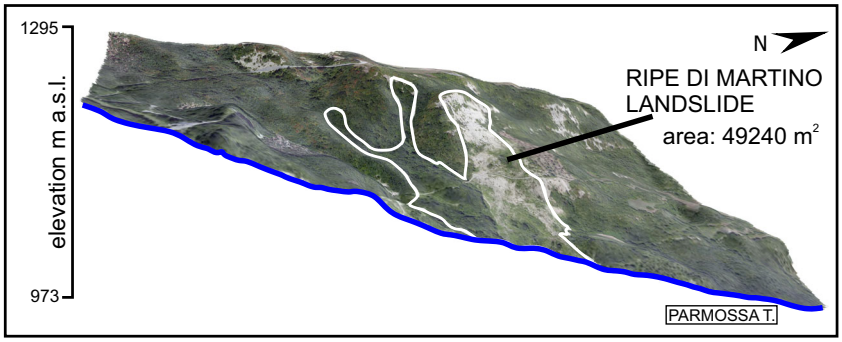

Fig. 7 3D diagram of the reactivated portion of the Ripe di Martino landslide occurred in 2000. Elevation is based on the 5-m-resolution DTM on which a Digitalglobe® freely available satellite image has been projected

the orientation of the tectonic lineaments highlighted by the DTM analysis. Also, the geophysical data related to the Musiara landslide confirm the existence of a tectonic control on the landslides development. In fact, the electrical resistivity tomography highlights the existence of rock rotational slides that developed along pre-existing SW-NE-oriented tectonic discontinuities and that have been, at least partially, reactivated by subsequent landslides. Moreover, the seismic profiles clearly show the presence of WNW-ESE-oriented high-angle discontinuities that controlled both the older rotational rockslides and the younger landslides that remobilize large portions of the previous ones (e.g. the last event of Musiara landslide). Therefore, it is possible to observe multiple generations of landslides, where the most recent ones partially or totally rework the older ones, even if controlled by the same structural elements.

This tectonic control can therefore be observed in the translational slides, like Carobbio, and in the complex landslides (roto-translational slides-earth/debris flows), like Musiara and Ripe di Martino. Within this framework, nonetheless, different tectonic processes affected the drainage basin development and, consequently, the hillslopes of the Parmossa and Parma valleys acquired different geometrical characteristics.

As highlighted by the geomorphometric analysis, the spatial distribution of anomalies in the used indices corresponds to zones of the Parmossa valley flanks characterized by an increasing degree of upstream incision, from N to S (Fig. 10). These areas are

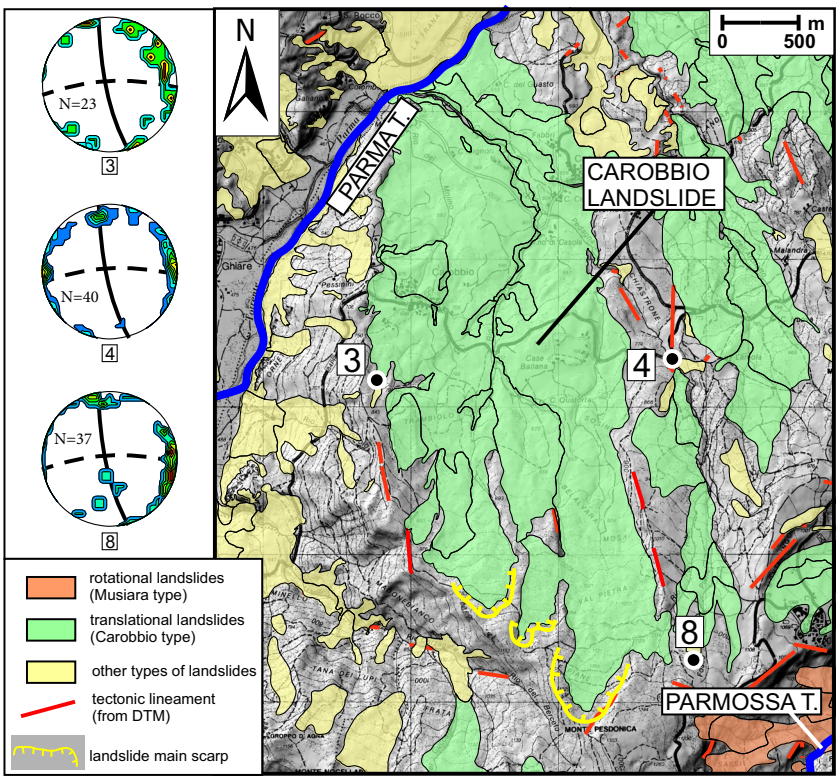

Fig. 8 Sketch map of the Carobbio landslide area. The *stereonets* represent the contours of the poles related to the joints orientation. *Black solid line* indicates orientation of the Ripe di Martino landslide flanks; *black dashed line* indicates orientation of the Ripe di Martino landslide scarp

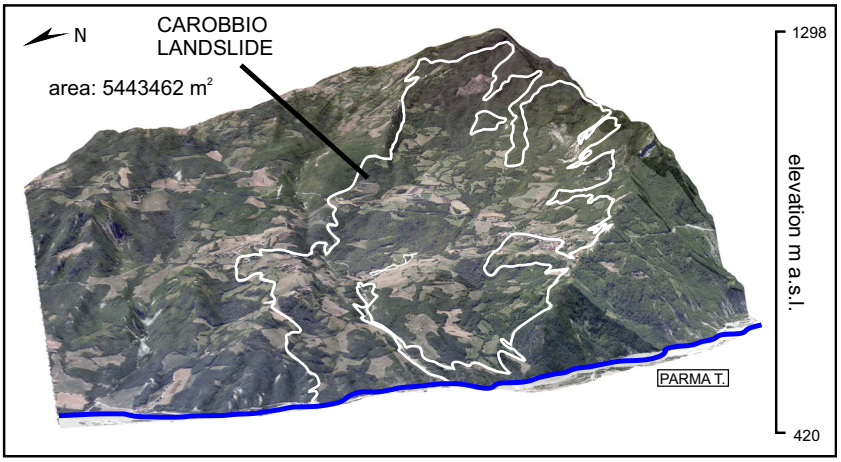

Fig. 9 3D diagram of the reactivated portion of the Carobbio landslide occurred in 2000. Elevation is based on the 5-m-resolution DTM on which a Digitalglobe® freely available satellite image has been projected

separated by NE-dipping normal faults that leave a progressively clearer signature on the topography from fault A to fault C (i.e. from N to S). Therefore, we hypothesise that the upper portion of the Parmossa valley has been affected by a progressive faulting process and subsequent upstream incision. The incision propagated from fault and area A (in which the incision is almost completely erased by shallow landslides such as flows), through fault and area B (where the incision is still clearly visible) up to fault and area C (where the fault is clearly visible and the incision is incipient, but not yet developed). The NE-dipping normal faults, located on the forelimb of the Ghiare antiform and following the orientation of the fold hinge, likely represent some of the shallow extensional tectonic features commonly affecting these contractional structures in this portion of the Northern Apennines. The erosion of the Parmossa Torrent, therefore, determined the incision of its thalweg, and caused an oversteepening and a reshaping of its valley slopes that led to the development of the Musiara-type landslides. The development of wider and less steep slopes (with respect to the Parmossa valley), instead, is related to the occurrence of Carobbio-type landslides.

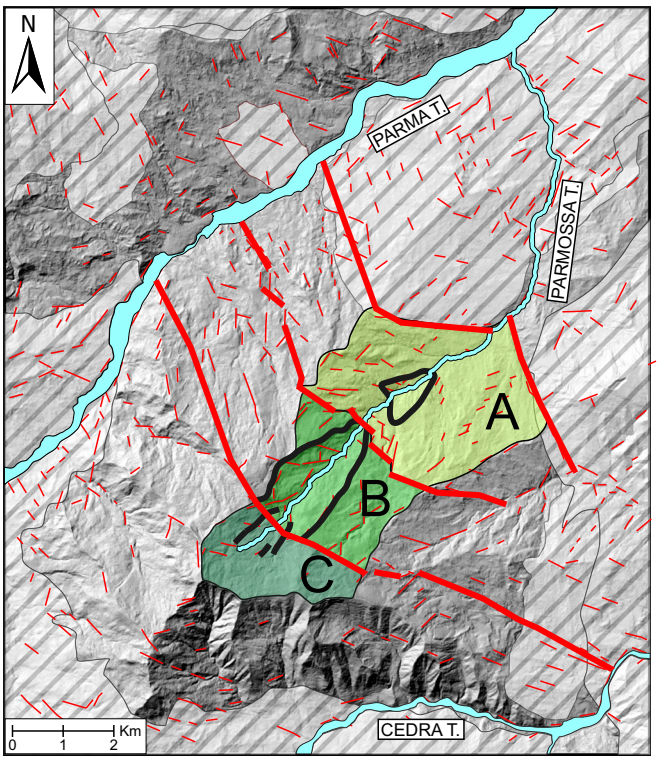

Fig. 10 DTM of the study area on which the faults and incised areas highlighted by the geomorphometric analysis along the Parmossa valley are represented. *Black solid lines* represent the portions of each single area in which evidences of enhanced valley incision are still preserved. *A*, *B* and *C* represent the faults and the relative (upstream) area of incision. See text for explanation. The *striped areas* represent lithologies different from the Mt. Caio flysch that are not considered in this study

The geomorphological evolution of the Parma and Parmossa valleys, even if different, is influenced in both cases by the tectonic activity of the aforementioned Ghiare antiform. The slope setting related to Carobbio-type landslides is produced mainly by the surface uplift of the whole antiform and the tilting of its forelimb, causing the subsequent steepening of the slope towards its threshold angle. In the case of the left side of the Parmossa valley, after a phase in which Carobbio-type landslides developed, the ongoing growth of the antiform possibly caused the activation of the normal faults and, in turn, of the torrent incision as geomorphic response, that favoured the development of Musiara-type landslides (Fig. 11).

This sequence of events, even if not constrained by absolute datings of the involved processes, is reasonably supported by the radiocarbon dating performed on the organic materials within the landslides deposits. In fact, the ages of the events of the Carobbio landslide are among the oldest in this portion of the Northern Apennines (Table 1), while the ages related to the Ripe di Martino landslide are significantly younger (Table 1, Soldati et al. 2006; Tellini and Chelli 2003). Even though it was not possible to find any organic material suitable for radiocarbon dating within the deposit of the Musiara landslide, the ages of the Ripe di Martino landslide events can be reasonably considered representative of the Musiara landslide too because they belong to the same landslide type and they developed during the same evolutionary phase.

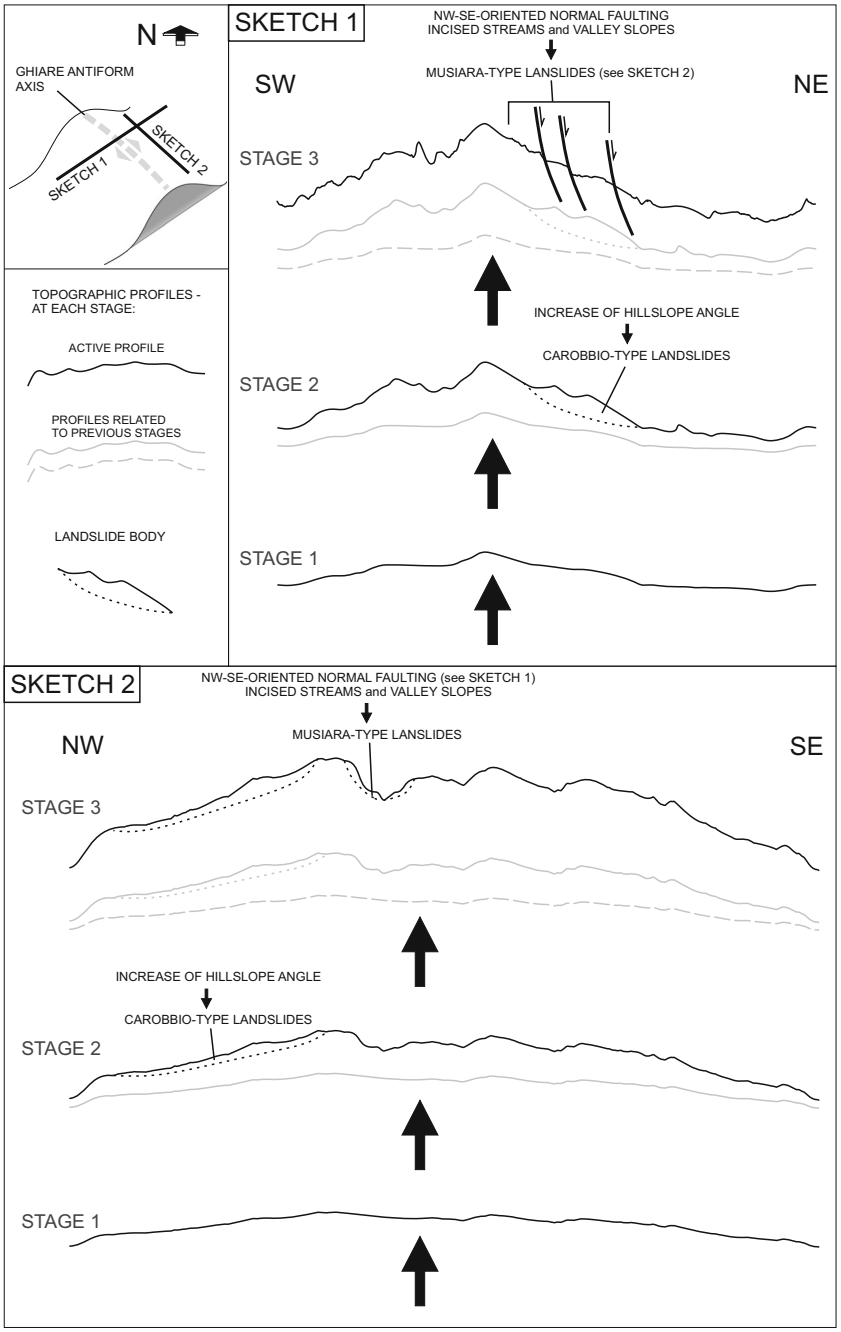

Fig. 11 Sketches showing the growth of Ghiare antiform (see Fig. 1) and the subsequent topographic and geomorphological response, i.e. development of prevailing translational (Carobbio-type) and rotational (Musiara-type) landslides. The *black solid lines* represent the topography active at each stage. The *grey solid lines* represent the topography related to a previous stage of the antiform growth (represented by *black arrows*)

This supports the hypothesis that Carobbio-type landslides developed during a phase in which the slope steepness was mainly controlled by the growth of the antiform. Instead, Musiara-type landslides represent the geomorphological result of the subsequent dissection of the antiform because of the activity of normal faults that caused the development of younger steeper slopes. In fact, Carobbio-type landslides generally occupy the higher section of the slopes, while Musiara-type landslides developed at the toe of the slopes, testifying, therefore, the existence of a more recent reshaping of the hillslopes (Fig. 1a).

The ages obtained from the Carobbio landslide (25129 ^{14}C year BP and 21200-20060 cal year BP) highlight how two of the landslide events occurred during the LGM. The proximity of the landslide to the principal glacier tongues suggests that the aforementioned periglacial processes acting during the last deglaciation phase reasonably contributed, in addition to tectonic processes, to the reshaping of the Parma valley slopes and to the promoting of the Carobbio landslide occurrence.

The two recognized types of landslides can be used as indicators of phases in which different tectonic and geomorphological

processes prevailed, basically because their differences and the causes of their occurrence are strictly connected to the differential tectonomorphic evolution of the hillslopes within the study area. The detailed understanding of these relationships highlights also the possibility to extend this kind of usage of landslide types to any active mountain belt in which tectonic processes are acting at a temporal scale comparable to the age of landslide activity and in which the lithologic and climatic conditions favour the development of landslides.

In this perspective, also the relative weight of geomorphological processes (landslides versus fluvial processes) in response to the tectonic processes affecting the study area may be differentiated through time. In particular, during the first phase, landsliding (Carobbio-type) seems to represent the prevailing surface expression of the Ghiare antiform growth, while during the second phase, stream erosion processes probably represent the most active response to tectonic forcing, and landslides (Musiara-type) represent the consequence of the fluvial processes affecting the hillslopes. Therefore, we envisage that landslide-oriented and fluvial incision-oriented models do not mutually exclude each other, and in our study area, even though more constraints are needed, both probably coexisted in an evolutionary scenario in which their relative contribution changed through the described phases.

Conclusions

We investigated in detail the different types of landslides and their relationships with the geomorphological and geological characters of the area. Tectonic features, lithology and bed attitude, which are homogeneous within the study area, mainly controlled the orientation of the landslides scarps and flanks, but do not seem to cause the occurrence of different types of landslides. This differentiation can be explained considering the evolution of the regional-scale antiformal structure that exerted different types of control on the hillslope evolution of the area. In particular, Carobbio-type landslides affected gently dipping slopes developed during the first phases of topographic growth of the Ghiare antiform. Subsequent phases of this growth led to the development of high-angle extensional faults dissecting the antiform and causing the streams to deeply incise their thalweg. This process produced more recent steep-dipping slopes on which Musiara-type landslides developed.

These different types of landslides, within the same geological framework, occurred in response to different geomorphological causes and phases of slope evolution. These considerations suggest also that our study area may represent an example in which landslide-dominated and fluvial incision-dominated models possibly coexisted, even though their relative weight in the geomorphological evolution of the area changed through time.

The results of this multidisciplinary work highlight the possibility, in active mountain belts where the geological, geomorphological and climatic framework is well constrained, to use landslides types as indicators of tectonic processes that, within the same area, may produce different types of hillslopes through time.

Acknowledgements

This paper has been funded to Alessandro Chelli by the University of Parma (FIL 2012 and FIL 2014) and by the Municipality of Lesignano de' Bagni (Parma—Italy).

The authors thank Dr. Andrea Ruffini (Servizio Pianificazione Territoriale—Trasporti, Parma Province Admin.) for the drone imagery of the Musiara landslide. The authors thank also the Editorial Board of Landslides and two anonymous reviewers for the helpful revision that greatly improved the first version of the manuscript.

M. Carlini, A. Chelli and R. Francese conceived the work and wrote the core of the paper. M. Carlini and S. Giacomelli performed the geomorphometric analysis. A. Chelli and C. Tellini performed the geomorphological analysis of the considered landslides and, with the contribution of M. Carlini, of the whole study area. R. Francese managed the geophysical data and the DTM of the Musiara landslide. R. Francese, M. Giorgi and A. Quagliarini produced the ERT while A. Carpena performed the seismic survey on the Musiara landslide.

References

Abbate E, Sagri M (1967) Suddivisioni litostratigrafiche nei calcari ad elmintoidi auctt. della placca dell'Ebro-Antola e correlazioni con terreni simili affioranti tra Voghera e Castelnovo ne' Monti (Appennino Settentrionale). Mem Soc Geol It 45:23–65

Ballantyne CK, Sandeman GF, Stone JO, Wilson P (2014) Rock-slope failure following Late Pleistocene deglaciation on tectonically stable mountainous terrain. Quat Sci Rev 86:144–157

Bertolini G, Pellegrini M (2001) The landslides of Emilia Apennines (northern Italy) with reference to those which resumed activity in the 1994-1999 period and required civil protection interventions. Quaderni di Geologia Applicata 8(1):27–74

Bertolini G, Guida M, Pizziolo M (2005) Landslides in Emilia-Romagna region (Italy): strategies for hazard assessment and risk management. Landslides 2(4):302–312

Bertolini G., Corsini A., Tellini C. (2017) Fingerprints of Large-Scale Landslides in the Landscape of the Emilia Apennines. In: Soldati M., Marchetti M. (eds) Landscapes and Landforms of Italy. World Geomorphological Landscapes. Springer, Cham, pp 215-224

Borgatti L, Corsini A, Barbieri M, Sartini G, Truffelli G, Caputo G, Puglisi C (2006) Large reactivated landslides in weak rock masses: a case study from the Northern Apennines (Italy). Landslides 3(2):115–124

Borgatti L, Soldati M (2010) Landslides as geomorphological proxy for climate change: a record from the Italian dolomites. Geomorphology 61:59–70

Burbank DW, Anderson RS (2011) Tectonic geomorphology. Blackwell Science, Oxford

Catane SG, Cabria HB, Tomarong CP, Saturay RM Jr, Zarco MAH, Pioquinto WC (2007) Catastrophic rockslide-debris avalanche at St. Bernard, Southern Leyte, Philippines. Landslides 4:85–90

Carlini M, Chelli A, Vescovi P, Artoni A, Clemenzi L, Tellini C, Torelli C (2016) Tectonic control on the development and distribution of large landslides in the Northern Apennines (Italy). Geomorphology 253:425–437

Centamore E, Ciccacci S, Del Monte M, Fredi P, Lupia Palmieri E (1996) Morphological and morphometric approach to the study of the structural arrangement of northeastern Abruzzo (central Italy). Geomorphology 16:127–137

Cerrina Feroni A, Ottria G, Vescovi P (a cura di) (2002) Note Illustrative della Carta Geologica d'Italia alla scala 1:50.000, foglio 217 "Neviano degli Arduini". Servizio Geologico d'Italia-Regione Emilia Romagna: S.EL.CA. srl, Firenze

Chelli A, Mandrone G, Truffelli G (2006) Field investigations and monitoring as tools for modelling the Rossena castle landslide (Northern Apennines, Italy). Landslides 3:252–259

Chigira M (2011) Geological and geomorphological characteristics of deep-seated catastrophic landslides induced by rain and earthquakes. J Chin Soil Water Conserv 42(4):265–278

Ciccacci S, D'alessandro L, Fredi P, Lupia Palmieri E (1992) Relation between morphometric characteristics and denudational processes in some drainage basins of Italy. Zeitschrift für Geomorphologie N.F. 36(1):53–67

Constable SC, Parker RL, Constable CG (1987) Occam's inversion: a practical algorithm for generating smooth models from electromagnetic sounding data. Geophysics 52(3):289–300

Crosta GB, Clague JJ (2006) Large landslides: dating, triggering, modelling, and hazard assessment. Eng Geol 83:1–3

Cruden DM, Varnes DJ (1996) Landslide types and processes. In: Turner AK, Shuster RL (eds) Landslides: investigation and mitigation, Transportation Research Board, National Research Council, special report, vol 247. National Academy Press, Washington DC, pp 36–75

Densmore AL, Hovius N (2000) Topographic fingerprint of bedrock landslides. Geology 28:371–374
Federici PR, Tellini C (1983) La geomorfologia dell'Alta Val Parma (Appennino Settentrionale). Riv Geogr It 90:393–428
Gao M, Zeilinger G, Xu X, Wang Q, Hao M (2013) DEM and GIS analysis of geomorphic indices for evaluating recent uplift of the northeastern margin of the Tibetan Plateau, China. Geomorphology 190:61–72
Giraudi C (2011) Middle Pleistocene to Holocene glaciations in the Italian Apennines. In: Ehlers J., Gibbard P.L., Hughes P.D. (Eds), Developments in Quat. Science. Vol. 15, – "Quaternary Glaciations - Extent and Chronology: A Closer Look", Elsevier B.V., pp 211-219
Hack JT (1973) Stream-profile analysis and stream-gradient index. U.S. Geolog Surv J Res 1:421–429
Hradecký J, Pánek T (2008) Deep-seated gravitational slope deformations and their influence on consequent mass movements (case studies from the highest part of the Czech Carpathians). Nat Hazards 45(2):235–253
Korup O, Densmore AL, Schlunneger F (2010) The role of landslides in mountain range evolution. Geomorphology 120:77–90
Larsen IJ, Montgomery DR (2012) Landslide erosion coupled to tectonics and river incision. Nat Geosci 5:467–473
Mandrone G (2004) Assessing of geomechanical features of some of the most common heterogeneous rock units in the Northern Apennines. Quaderni di Geologia Applicata 11:5–18
Margielewski W (2006) Structural control and types of movements of rock mass in anisotropic rocks: case studies in the Polish Flysch Carpathians. Geomorphology 77:47–68
McColl ST (2012) Paraglacial rock-slope stability. Geomorphology 153-154:1–16
Morelli G, Labrecque DJ (1996) Advances in ERT modelling. Eur J Environ Eng Geophys 1(2):171–186
Mumipour M, Tahmasabi Nejad H (2011) Tectonics geomorphology settings of Khatiz anticline derived from GIS processing, Zagros Mountains, Iran. Asian J Earth Sci 4(3):171–182
Oldenburg DW, Li Y (1999) Estimating depth of investigation in dc resistivity and IP surveys. Geophysics 64(2):403–416
Pánek T, Hradecký J, Šilhán K (2008) Application of electrical resistivity tomography (ERT) in the study of various types of slope deformations in anisotropic bedrock: case studies from the Flysch Carpathians. Studia Geomorphologica Carpatho-Balcanica 17:57–73
Perego S, Vescovi P (1991) Osservazioni morfotettoniche e idrografiche in media Val Parma (Appennino settentrionale). Mem Descr Carta Geol D'It 46:487–496
Roering J (2012) Tectonic geomorphology: landslides limit mountain relief. Nat Geosci 5:446–447
Servizio Geologico, Sismico e dei Suoli della Regione Emilia-Romagna (2014) - Carta Inventario delle frane a scala 1:10000 della Regione Emilia-Romagna
Shahzad F, Gloaguen R (2011) TecDEM: a MATLAB based toolbox for tectonic geomorphology, part 2: surface dynamics and basin analysis. Comput Geosci 37(2):261–271
Šilhán K, Pánek T, Turský O, Brázdil R, Klimeš J, Kašičková L (2014) Spatio-temporal patterns of recurrent slope instabilities affecting undercut slopes in flysch: a dendrogeomorphic approach using broad-leaved trees. Geomorphology 213:240–254
Soldati M, Borgatti L, Cavallin A, De Amicis M, Frigerio S, Giardino M, Mortara G, Pellegrini GB, Ravazzi C, Surian N, Tellini C, Zanchi A, Alberto W, Albanese D, Chelli A, Corsini A, Marchetti M, Palomba M, Panizza M (2006) Geomorphological evolution of slopes and climate changes in northern Italy during the late quaternary: spatial and temporal distribution of landslides and landscape sensitivity implications. Geogr Fis Din Quat 29(2):165–183 Issn:0391–9838
Tellini C, Chelli A (2003) Ancient and recent landslide occurrences in the Emilia Apennines (Northern Apennines, Italy). In: Castaldini D, Gentili B, Materazzi M, Pambianchi G (eds) Proc. Workshop on "Geomorphological sensitivity and system response", Camerino—Modena Apennines (Italy), July 4th – 9th, 2003, pp 105–114
Tosatti G, Castaldini D, Barbieri M, D'Amato Avanzi G, Giannecchini R, Mandrone G, Pellegrini M, Perego S, Puccinelli A, Romeo RW, Tellini C (2008) Additional causes of seismically-related landslides in the northern Apennines. Italy Revista Geomorf 10:5–21
Troiani F, Della Seta M (2008) The use of the stream length-gradient index in morphotectonic analysis of small catchments: a case study from Central Italy. Geomorphology 102:159–168
Vesnaver A (2013) Seismic tomography from the old to the new millennium. Arab J Sci Eng 38(1):1–9
Záruba Q (1922) Study on landslide terrains in the Vsetín and Vallachian region. Práce z geologického ústavu čes vys učení technického v Praze 170–177

Electronic supplementary material The online version of this article (doi:10.1007/s10346-017-0871-2) contains supplementary material, which is available to authorized users.

M. Carlini · A. Chelli (✉) · R. Francese · S. Giacomelli · A. Quagliarini · C. Tellini
Department of Chemistry, Life Sciences and Environmental Sustainability,
University of Parma,
Parco Area delle Scienze, 157/A, 43124, Parma, Italy
e-mail: alessandro.chelli@unipr.it

M. Carlini · S. Giacomelli
Dipartimento di Scienze Biologiche, Geologiche ed Ambientali-BiGeA,
University of Bologna,
Via Zamboni, 33, 40126, Bologna, Italy

R. Francese · M. Giorgi
National Institute of Oceanography and Experimental Geophysics-OGS,
Borgo Grotta Gigante 42/C, 34010, Sgonico, Trieste, Italy

A. Carpena
GEOREFLEX s.r.l,
via Carlo Fioruzzi 15, 29121, Piacenza, Italy